Electronic Supplementary Material (ESI) for Journal of Materials Chemistry A.
This journal is © The Royal Society of Chemistry 2019

Supporting Information

Two–Dimensional π–Conjugated Metal Bis(Dithiolene) Nanosheets as Promising Electrocatalysts for Carbon Dioxide Reduction: A Computational Study

Yu Tian,[a] Changyan Zhu,[a] Likai Yan,[a*] Jingxiang Zhao,[b*] and Zhongmin Su[a]

[a] Institute of Functional Materials Chemistry and National & Local United Engineering Lab for Power Battery, Faculty of Chemistry, Northeast Normal University, Changchun, 130024, China.

[b] College of Chemistry and Chemical Engineering, Harbin Normal University, Harbin, 150025, China.

* To whom correspondence should be addressed. *E*–mail: yanlk924@nenu.edu.cn (L. K.); xjz_hmily@163.com (J. –X. Zhao).

Table S1. The geometric parameters, charge (Q)[a] of per M atom, magnetic moment of per M atom (M_M) [a] and total moment of $M_3C_{12}S_{12}$ (M_{tot}) [a].

	lattice constant (Å)	M−S distance (Å)	Q (e)	$M_M(\mu_B)$	M_{tot} (μ_B)	E_{coh}/eV
$Fe_3C_{12}S_{12}$	14.80	2.19	0.70	2.16	5.86	–5.25
$Co_3C_{12}S_{12}$	14.76	2.17	0.58	0.98	2.90	–5.19
$Ni_3C_{12}S_{12}$	14.62	2.15	0.51	0.00	0.00	–5.24
$Ru_3C_{12}S_{12}$	15.19	2.29	0.55	1.49	4.84	–5.31
$Rh_3C_{12}S_{12}$	15.07	2.27	0.36	0.26	1.03	–5.28
$Pd_3C_{12}S_{12}$	15.05	2.30	0.30	0.00	0.00	–5.07

[a]The Bader charge and magnetic momentum are calculated by VASP program.

Table S2. The computed free energies (ΔG) of CO_2RR species on $Ru_3C_{12}S_{12}$ and $Rh_3C_{12}S_{12}$ sheets.

	Elementary Step	ΔG/eV
$Ru_3C_{12}S_{12}$	$CO^* \rightarrow CO + *$	1.78
$Ru_3C_{12}S_{12}$	$CO^* + H^+ + e^- \rightarrow CHO^*$	1.08
$Rh_3C_{12}S_{12}$	$CO^* \rightarrow CO + *$	0.99
$Rh_3C_{12}S_{12}$	$CO^* + H^+ + e^- \rightarrow CHO^*$	0.43
$Rh_3C_{12}S_{12}$	$CO^* + H^+ + e^- \rightarrow COH^*$	1.82
$Rh_3C_{12}S_{12}$	$CHOH^* + H^+ + e^- \rightarrow CH^* + H_2O$	0.88
$Rh_3C_{12}S_{12}$	$CHO^* + H^+ + e^- \rightarrow H_2CO^*$	0.64

Table S3. Chemical process and transition state imaginary vibrational frequency for each elementary step on $Rh_3C_{12}S_{12}$.

Elementary Step	**Chemical process**	**TS *Vib.* (cm^{-1})**
$CO_2 + H^* \rightarrow COOH^*$	O–H bond formation	*i* 894.18
$COOH^* + H^* \rightarrow CO^* + H_2O$	C–OH bond dissociation with O–H bond formation	*i* 1150.65
$CO^* + H^* \rightarrow CHO^*$	C–H bond formation	*i* 1687.28
$CHO^* + H^* \rightarrow CHOH^*$	O–H bond formation	*i* 1381.83
$CHO^* + H^* \rightarrow H_2CO^*$	C–H bond formation	*i* 273.15
$CHOH^* + H^* \rightarrow CH_2OH^*$	C–H bond formation	*i* 1568.20
$H_2CO^* + H^* \rightarrow OCH_3^*$	C–H bond formation	*i* 1418.47
$CH_2OH^* + H^* \rightarrow CH_2^*(bri) + H_2O$	C–OH bond dissociation with O–H bond formation	*i* 355.33
CH_2^* (bri) + $H^* \rightarrow CH_2^*$(top)	C–S bond dissociation	*i* 216.88
$OCH_3^* + H^* \rightarrow CH_3OH^*$	C–H bond formation	*i* 1352.04
$CH_2^* + H^* \rightarrow CH_3^*$	C–H bond formation	*i* 1312.34
$CH_3^* + H^* \rightarrow CH_4 + *$	C–H bond formation	*i* 1039.79

Table S4. Chemical process and transition state imaginary vibrational frequency of water–assisted CHO^* formation on $Rh_3C_{12}S_{12}$.

Elementary Step	Model	Chemical process	TS *Vib.* (cm^{-1})
$CO^* + H^* \rightarrow CHO^*$	H–shuttling	C–H bond formation	*i* 773.03
$CO^* + H^* \rightarrow CHO^*$	water–solvated	C–H bond formation	*i* 1678.86

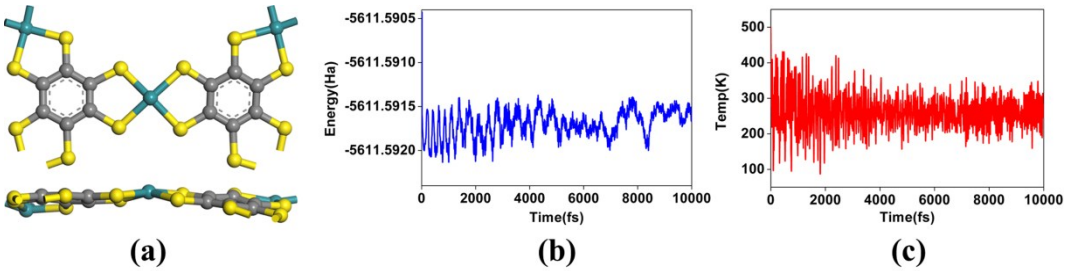

Figure S1. (a) Geometry snapshot, variation of (b) total energy and (c) temperature of $Ru_3C_{12}S_{12}$ at 10 ps during MD simulation at 500 K.

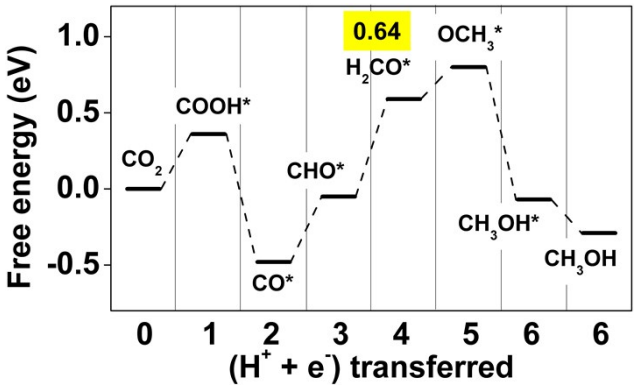

Figure S2 Free energy profiles for reduction CO_2 to CH_3OH formation on $Rh_3C_{12}S_{12}$. The pathway is shown at the indicated potential of 0 V vs RHE. The free energy zero is set as that of the catalyst and the isolated CO_2 molecule. The maximum ΔG of the whole pathway is highlighted in yellow.

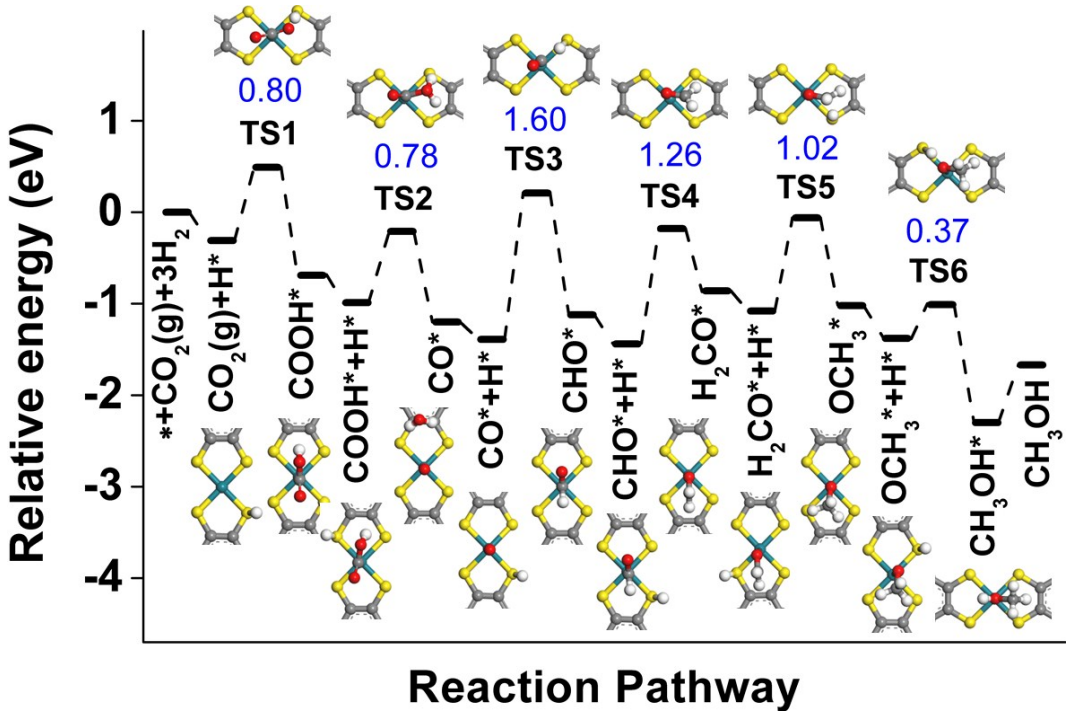

Figure S3 Potential energy profiles for reduction CO_2 to CH_3OH on $Rh_3C_{12}S_{12}$. The total energy of the catalyst, isolated CO_2, and three H_2 are taken as zero for reference. Color code: Rh, green; S, yellow; C, gray; O, red; H, white.

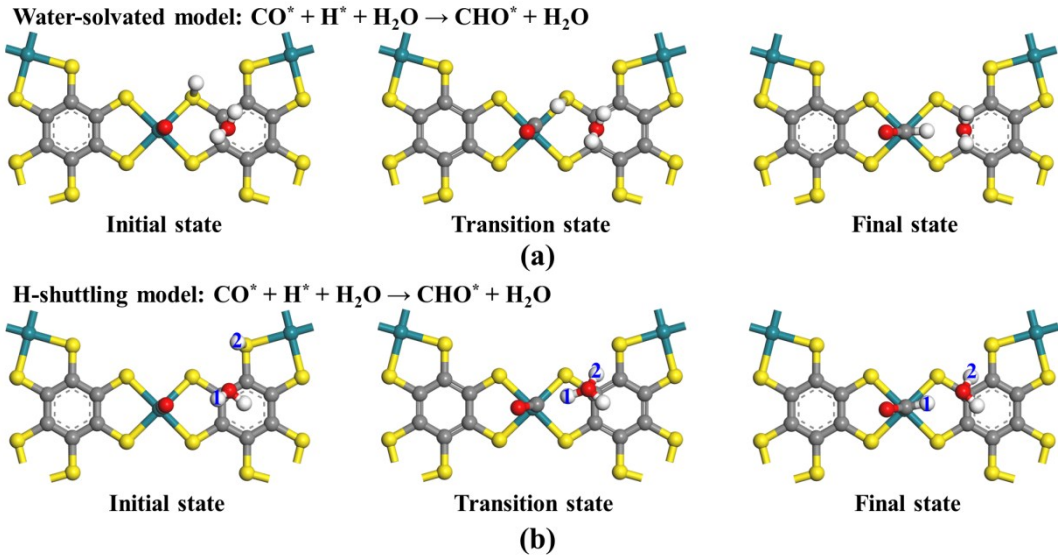

Figure S4 The structures of the initial, transition, and final states for reduction CO^* to CHO^* on $Rh_3C_{12}S_{12}$ with 1 H_2O in the (a) water−solvated, and (b) H−shuttling models.

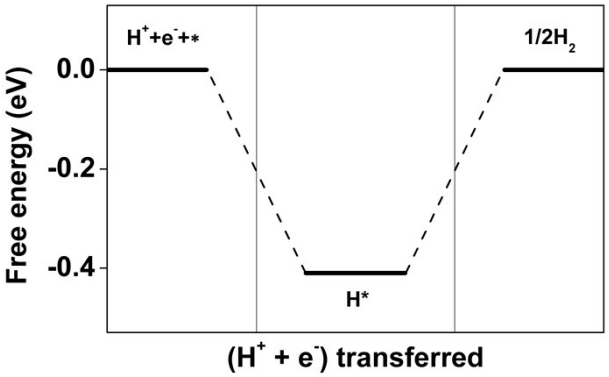

Figure S5. The energy diagram of the HER on $Rh_3C_{12}S_{12}$.